

ARTICLE OPEN



IGF2BP2-modified circular RNA circARHGAP12 promotes cervical cancer progression by interacting m⁶A/FOXO1 manner

Fei Ji^{1,2,5}, Yang Lu^{1,5}, Shaoyun Chen³, Yan Yu¹, Xiaoling Lin⁴, Yuanfang Zhu¹✉ and Xin Luo^{2,4}✉

© The Author(s) 2021

Emerging evidence indicates that circular RNA (circRNA) and N⁶-methyladenosine (m⁶A) play critical roles in cervical cancer. However, the synergistic effect of circRNA and m⁶A on cervical cancer progression is unclear. In the present study, our sequencing data revealed that a novel m⁶A-modified circRNA (circARHGAP12, hsa_circ_0000231) upregulated in the cervical cancer tissue and cells. Interestingly, the m⁶A modification of circARHGAP12 could amplify its enrichment. Functional experiments illustrated that circARHGAP12 promoted the tumor progression of cervical cancer in vivo and vitro. Furthermore, MeRIP-Seq illustrated that there was a remarkable m⁶A site in FOXO1 mRNA. CircARHGAP12 interacted with m⁶A reader IGF2BP2 to combine with FOXO1 mRNA, thereby accelerating the stability of FOXO1 mRNA. In conclusion, we found that circARHGAP12 exerted the oncogenic role in cervical cancer progression through m⁶A-dependent IGF2BP2/FOXO1 pathway. These findings may provide new concepts for cervical cancer biology and pathological physiology.

Cell Death Discovery (2021)7:215; <https://doi.org/10.1038/s41420-021-00595-w>

INTRODUCTION

Cervical cancer is the second most frequent malignant cancer for women worldwide and the third primary cause of cancer-related death in developing countries [1, 2]. Although the increasing application of cervical smear screening and the cervical cancer vaccine make the mortality and morbidity of cervical cancer decreasing, the molecular mechanism underlying cervical cancer is not entirely explicit [3]. In view of this situation, the therapeutic effect for cervical cancer is dissatisfied, we should pay attention to the targeted therapy tracking the pathogenesis.

Circular RNAs (circRNAs) are a group of non-coding RNA without protein-coding ability [4, 5]. More and more researches found that deregulated levels of circRNAs are involved in the initiation and progression of cervical cancer [6, 7]. For example, a representative circRNA circ-ITCH is lowly expressed in cervical cancer tissues and cells. Overexpression of circ-ITCH significantly suppresses the cellular proliferation, migration/invasion through sponging miRNA-93-5p, and regulating the expression of FOXK2 [8]. Moreover, upregulated circRNA hsa_circRNA_101996 serves as a miR-8075 sponge to target TPX2 in cervical cancer, thereby promoting cervical cancer proliferation and invasion [9]. Therefore, these data suggests that circRNA might function as an oncogenic or anticancer element.

N⁶-methyladenosine (m⁶A) is the most abundant RNA modification occurring in eukaryotic mRNAs [10]. m⁶A modification is a dynamic and reversible process mediated by two types of catalytic enzymes, including m⁶A writer (METTL3, METTL14, KIAA1429, and WTAP) and eraser (FTO, ALKBH5) [11–13]. Besides, another m⁶A

enzymes (m⁶A readers) could regulate the fate of m⁶A-containing mRNAs, including nuclear, export, mRNA stability, and mRNA translation. It has been identified that m⁶A could regulate tumorigenic progression. For example, m⁶A methyltransferase METTL3 is significantly upregulated in cervical cancer tissue and cells and promotes the proliferation, Warburg effect (aerobic glycolysis) through targeting the 3'-UTR of HK2 mRNA to enhance HK2 stability [14]. Moreover, YTHDF1/eEF-2 complex and IGF2BP3 positively promote the translation elongation and mRNA stability of pyruvate dehydrogenase kinase 4 (PDK4) to regulate glycolysis of cervical cancer cells [15]. Thus, these findings suggest that m⁶A might act as an essential regulator in cervical cancer progression.

In this study, we performed the circRNA microarray analysis in cervical cancer and results demonstrated that a novel circARHGAP12 (hsa_circ_0000231) was significantly upregulated in the cervical cancer tissue and cells. CircARHGAP12 was 794 bp length and generated from exon 3 and exon 2 in the ARHGAP12 gene. Our research found that circARHGAP12 could enhance the stability of FOXO1 mRNA via binding with IGF2BP2. Thus, our data suggest that circARHGAP12/m⁶A/IGF2BP2/FOXO1 axis in the cervical cancer tumorigenesis.

RESULTS

circARHGAP12 was an unfavorable circRNA for cervical cancer

Using the circRNA microarray analysis, we found that there were hundreds of circRNAs varied within the cervical cancer tissue and adjacent normal tissue (Fig. 1A, B). One of the new molecules that

¹Department of Obstetrics and Gynecology, Shenzhen Baoan Women's and Children's Hospital, Jinan University, Shenzhen 518102, China. ²The First Clinical Medical College of Jinan University, Guangzhou 510632, China. ³Maternal-Fetal Medicine Institute, Shenzhen Baoan Women's and Children's Hospital, Jinan University, Shenzhen 518102, China.

⁴Department of Obstetrics and Gynecology, The First Affiliated Hospital of Jinan University, Guangzhou 510632, China. ⁵These authors contributed equally: Fei Ji, Yang Lu.

✉email: zhuyfdoctor@sina.com; doctor_luoxin.edu@aliyun.com

Edited by Ivano Amelio

Received: 11 June 2021 Revised: 10 July 2021 Accepted: 26 July 2021

Published online: 14 August 2021

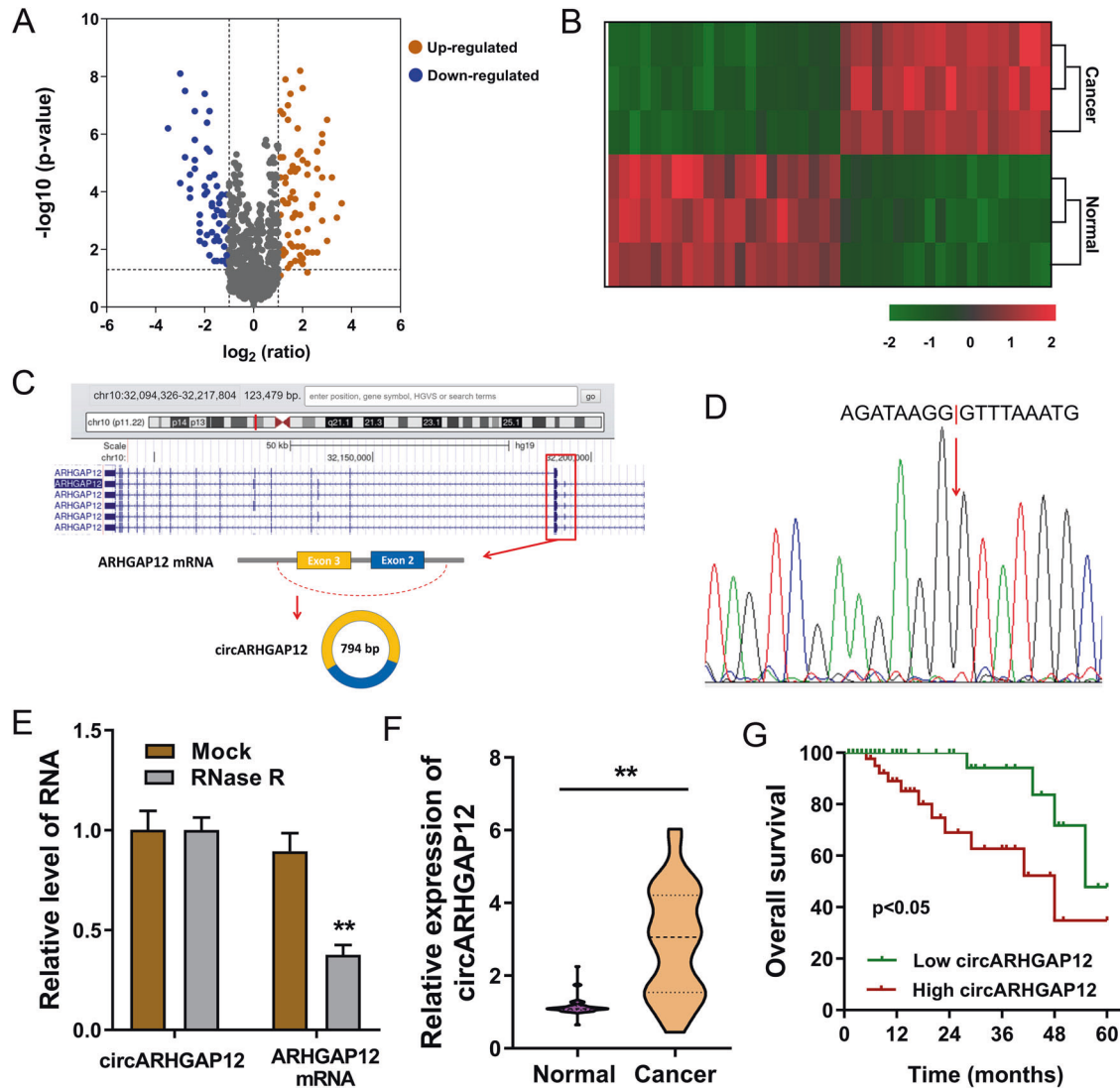


Fig. 1 **circARHGAP12** was an unfavorable circRNA for cervical cancer. **A** Volcano plot of circRNA microarray analysis revealed the down-regulated circRNAs within the cervical cancer tissue and adjacent normal tissue. **B** Heatmap of circRNA microarray analysis. **C** Schematic diagram demonstrated the generation of circARHGAP12 (hsa_circ_0000231, 796-bp) from exon-3 and exon-2 of ARHGAP12 gene through back splicing. **D** Sanger sequencing revealed the conjunction sites of circARHGAP12 back splicing. **E** RNA persistence testing using RNase R showed the expression of circular transcript (circARHGAP12) and linear mRNA (ARHGAP12 mRNA) detected using RT-PCR. **F** In the collected cervical cancer specimens' group, circARHGAP12 expression was analyzed using RT-PCR. **G** Survival analysis using the Kaplan–Meier survival curve and the log-rank test demonstrated the survival rate of patients with higher or lower circARHGAP12 levels. P values were calculated by Student's *t*-test. ** $p < 0.01$.

attracted our attention was circARHGAP12 (hsa_circ_0000231, 796-bp). CircARHGAP12 was generated from the exon-3 and exon-2 of the ARHGAP12 gene through back splicing (Fig. 1C). Sanger sequencing found that the conjunction sites of circARHGAP12 back splicing was in line with the prediction sites (Fig. 1D). In the RNA persistence testing using RNase R or control group, RT-PCR analysis found that the circular transcript, rather than linear mRNA, was much resistant to enzymatic digestion (Fig. 1E). In the collected cervical cancer specimens' group, we found that the expression of circARHGAP12 was much higher as compared to the adjacent normal tissue (Fig. 1F and Table 1). Survival analysis using Kaplan–Meier survival curve and the log-rank test demonstrated that the survival rate of patients with higher circARHGAP12 level was lower than the lower patients with statistical significance (Fig. 1G). These results are consistent with the finding that circARHGAP12 was an unfavorable circRNA for cervical cancer.

m⁶A modification of circARHGAP12 could increase its stability

As shown in the figure, the expression of circARHGAP12 was detected using RT-PCR, and data showed that circARHGAP12 expression was upregulated in the cervical cancer cells (Fig. 2A). The m⁶A enrichment in the cervical cancer cells was higher than the normal cells (Fig. 2B). MeRIP-PCR found that the circARHGAP12 enrichment was higher in the anti-m⁶A immunoprecipitation in cervical cancer (CaSki, SiHa) (Fig. 2C). We found that circARHGAP12 could interact with the specific m⁶A reader IGF2BP2 (Fig. 2D). RNA stability assay illustrated that, in the IGF2BP2 over-expression group, the circARHGAP12 level was slightly higher than the control group (Fig. 2E). Moreover, MeRIP-PCR assay data revealed that the IGF2BP2 overexpression promoted the circARHGAP12 expression in cervical cancer (CaSki, SiHa) (Fig. 2F). Thus, these findings suggested that m⁶A-modified circARHGAP12 could increase its stability.

circARHGAP12 promoted the tumorigenesis of cervical cancer

To address whether circARHGAP12 could regulate the tumorigenesis of cervical cancer, the overexpression and knockdown of circARHGAP12 were constructed using stable transfection (Fig. 3A). CCK-8 proliferation assay demonstrated that circARHGAP12 overexpression accelerated the proliferative ability of

cervical cancer cells (CaSki), and the knockdown of circARHGAP12 repressed the proliferation of cervical cancer cells (SiHa) (Fig. 3B). Transwell migration assay illustrated that circARHGAP12 promoted the migration of cervical cancer cells (CaSki), and the knockdown of circARHGAP12 inhibited the migration of cervical cancer cells (SiHa) (Fig. 3C). Colony formation assays displayed that circARHGAP12 overexpression enhanced the colony formation and knockdown of circARHGAP12 restrained the clones of cervical cancer cells (Fig. 3D). In vivo mice assay found that the transfection of circARHGAP12 overexpression (CaSki cells) could promote the in vivo tumor growth (Fig. 3E). In summary, these data suggested that circARHGAP12 promoted the tumorigenesis of cervical cancer.

Table 1. The correlations between circARHGAP12 and cervical cancer patients' clinicopathological characteristics.

	N (48)	circARHGAP12		P
		Low (24)	High (24)	
Age				
<45 year	22	10	12	0.415
≥45 year	26	14	12	
Tumor size				
<4 cm	21	14	7	0.013*
≥4 cm	27	10	17	
FIGO stages				
I/II	25	12	13	0.247
III/IV	23	12	11	
Tumor differentiation				
Well/moderate	30	11	19	0.153
Poor	18	13	5	
Lymph node metastasis				
Positive	17	10	7	0.139
Negative	31	14	17	

*indicate the $p < 0.05$.

circARHGAP12 interacted with m⁶A reader IGF2BP2

With the help of bioinformatics prediction, we found that circARHGAP12 might interact with the RNA binding protein (RBP) IGF2BP1 and IGF2BP2 (<https://circinteractome.nia.nih.gov/>, <http://rbpdb.cbr.utoronto.ca/>) (Fig. 4A). RBP immunoprecipitation (RIP) assay demonstrated that circARHGAP12 was enriched in the anti-IGF2BP2 antibody group, suggesting the molecular interaction within circARHGAP12 and IGF2BP2 (Fig. 4B). Fluorescence in situ hybridization (FISH) assay illustrated that circARHGAP12 distributed in the cytoplasm of cervical cancer (CaSki) cells, and IGF2BP2 disperse both in the nucleus and cytoplasm (Fig. 4C). Moreover, a pull-down assay was performed and RT-qPCR results found that the enrichment of circARHGAP12 was prominently enriched in the circARHGAP12 probe group as compared to the control probe group (Fig. 4D, E left). Besides, the western blot assay found that IGF2BP2 protein was enriched in the circARHGAP12 probe group (Fig. 4D, E right). Taken together, these findings concluded that circARHGAP12 interacted with m⁶A reader IGF2BP2.

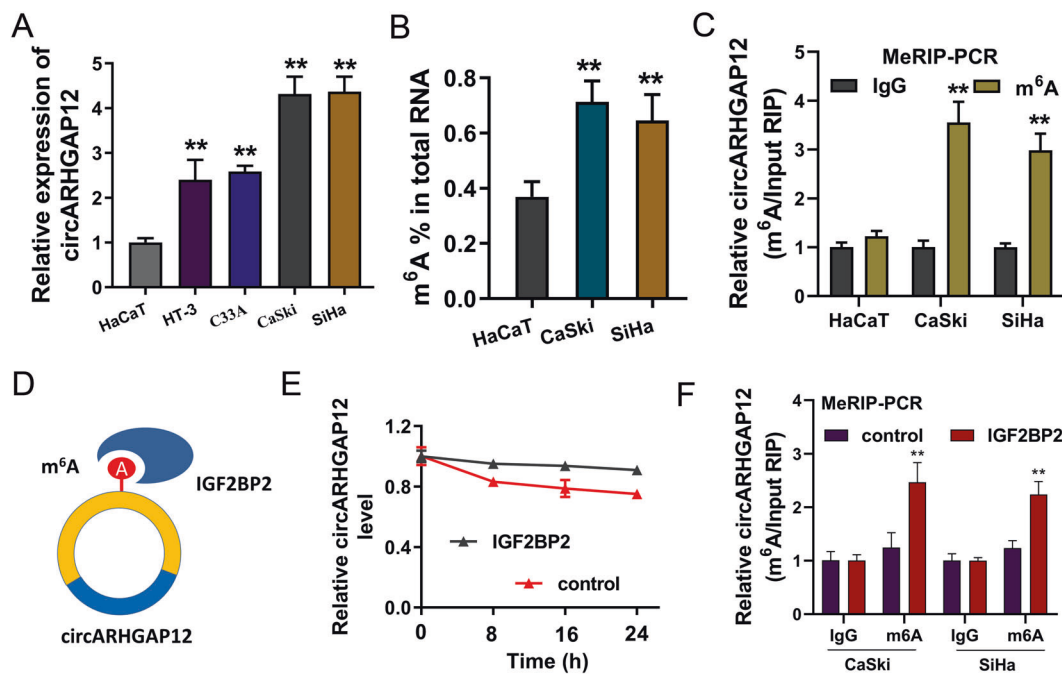


Fig. 2 m⁶A modification of circARHGAP12 could increase its stability. **A** RT-PCR showed the circARHGAP12 expression in the cervical cancer cells (HT-3, CaSki, C33A, and SiHa). **B** m⁶A quantitative analysis detected the m⁶A enrichment in the cervical cancer cells (CaSki and SiHa) and normal cells (HaCaT). **C** MeRIP-PCR detected the circARHGAP12 enrichment in anti-m⁶A immunoprecipitation in cervical cancer (CaSki and SiHa) and normal cells (HaCaT). **D** Schematic diagram displayed the interaction within circARHGAP12 and IGF2BP2. **E** RNA stability assay illustrated the circARHGAP12 level in the IGF2BP2 overexpression group and control group. **F** MeRIP-PCR assay measured the circARHGAP12 expression in cervical cancer (CaSki, SiHa) transfected with IGF2BP2 overexpression. Experiments were performed in triplicate. *P* values were calculated by Student's *t*-test. ** $p < 0.01$.

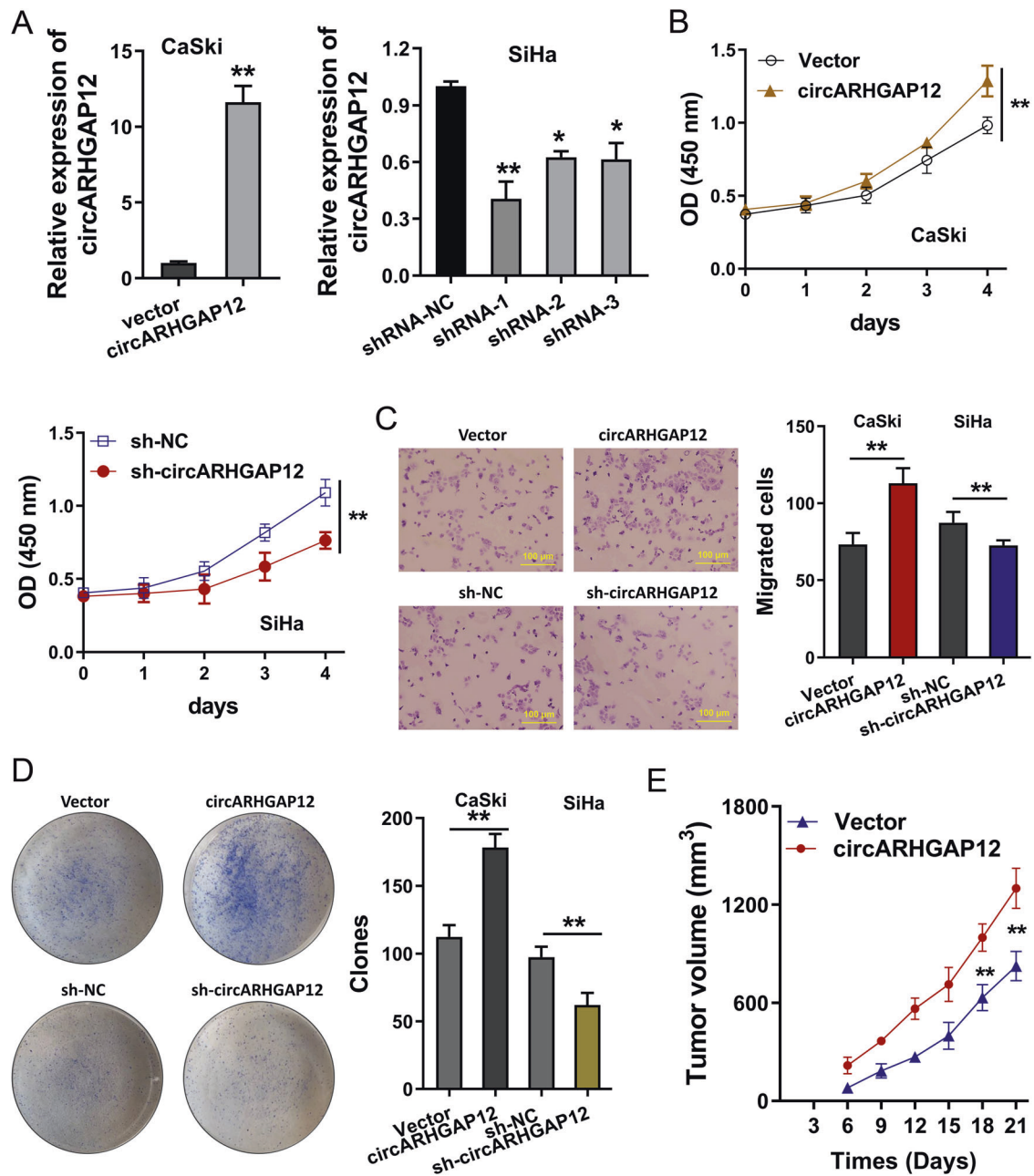


Fig. 3 circARHGAP12 promoted the tumorigenesis of cervical cancer. **A** Overexpression and knockdown of circARHGAP12 were constructed using stable transfection. Expression of circARHGAP12 was detected using RT-qPCR. **B** CCK-8 proliferation assay demonstrated the proliferative ability of cervical cancer cells (CaSki and SiHa) respectively transfected with circARHGAP12 knockdown (sh-circARHGAP12) and circARHGAP12 overexpression (circARHGAP12). **C** Transwell migration assay illustrated the migration of cervical cancer cells (CaSki and SiHa) transfected with circARHGAP12 knockdown (sh-circARHGAP12) and circARHGAP12 overexpression (circARHGAP12). **D** Colony formation assays displayed the colony formation of cervical cancer cells. **E** In vivo mice assay found the tumor growth in mice injected of circARHGAP12 overexpression cells (CaSki cells). Experiments were performed in triplicate. *P* values were calculated by Student's *t*-test. ***p* < 0.01.

circARHGAP12/IGF2BP2 enhanced the stability of FOXM1 mRNA

MeRIP-Seq was performed to discover the potential m⁶A modification profile in the cervical cancer cells (Fig. 5A). Sequencing data demonstrated that the m⁶A sites' enrichment was displayed in the connection point of 5'-UTR or 3'-UTR and CDS. Evidences had revealed the critical role of FOXM1 in cervical cancer. Coincidentally, MeRIP-Seq found that there was a remarkable m⁶A modification site in the 3'-UTR of FOXM1 mRNA (Fig. 5B). The m⁶A motif in the FOXM1 mRNA was found to be GGACU (Fig. 5C). RIP qPCR assay demonstrated that circARHGAP12 overexpression could improve

the FOXM1 mRNA enrichment precipitated by anti-IGF2BP2 antibody in the CaSki cells, and circARHGAP12 knockdown reduced the FOXM1 mRNA enrichment precipitated by anti-IGF2BP2 antibody in the SiHa cells (Fig. 5D). RNA stability assay and western blot assay revealed that circARHGAP12 overexpression promoted the FOXM1 mRNA stability (Fig. 5E down) and FOXM1 protein level (Fig. 5E up). Moreover, RNA stability assay indicated that IGF2BP2 overexpression enhanced the FOXM1 mRNA stability (Fig. 5F left), and IGF2BP2 silencing reduced the FOXM1 mRNA stability (Fig. 5F Right). In conclusion, the above data suggested that circARHGAP12/IGF2BP2 enhanced the stability of FOXM1 mRNA.

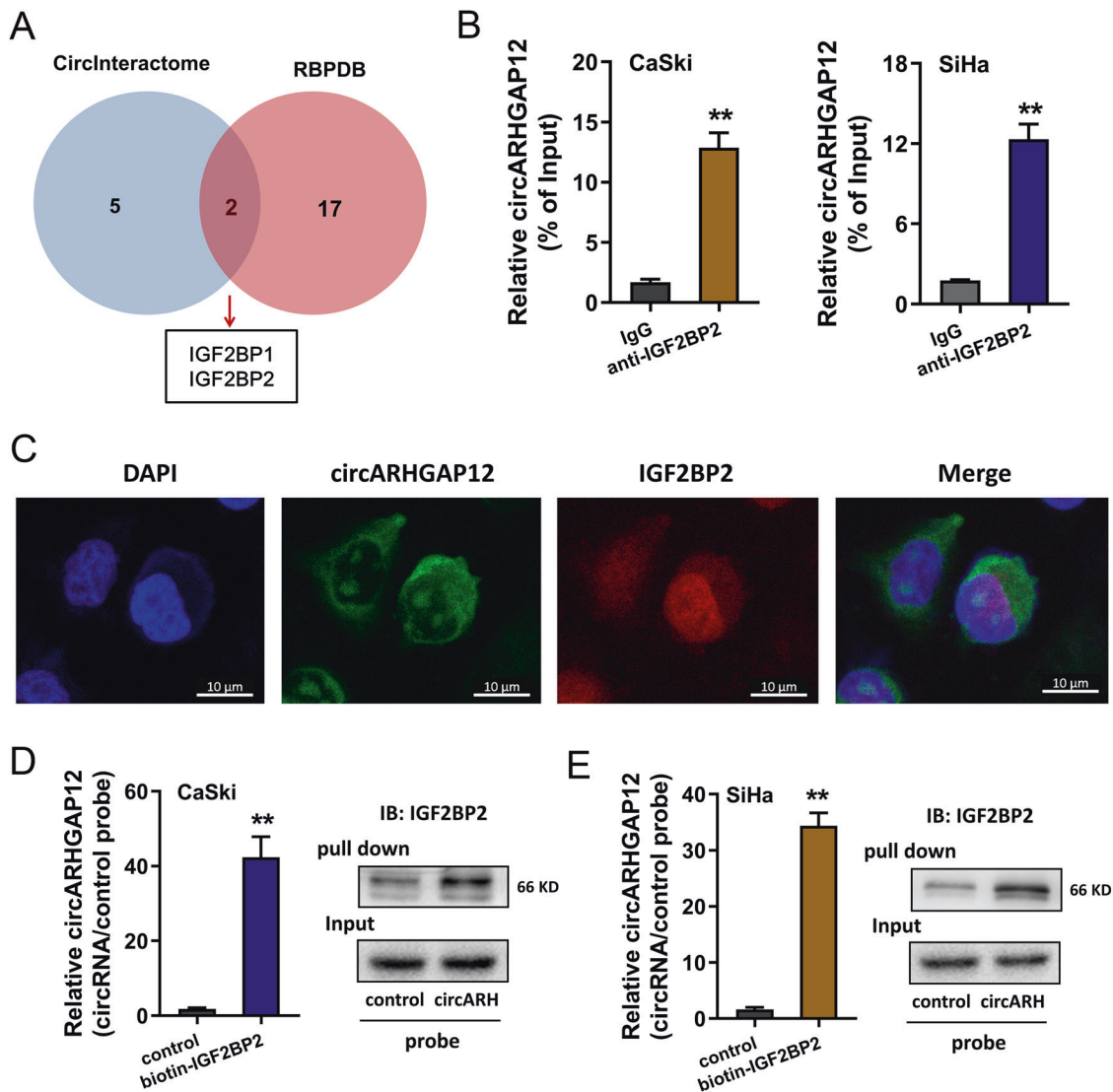


Fig. 4 circARHGAP12 interacted with m⁶A reader IGF2BP2. **A** Online bioinformatics tool (<https://circinteractome.nia.nih.gov/>, <http://rbpdb.cbr.utoronto.ca/>) found that circARHGAP12 might interact with the RNA binding protein (RBP) IGF2BP1 and IGF2BP2. **B** RBP immunoprecipitation (RIP) assay following qPCR demonstrated the enrichment of circARHGAP12 in the anti-IGF2BP2 or IgG antibody group (CaSki, SiHa). **C** Fluorescence in situ hybridization (FISH) assay illustrated the distribution of circARHGAP12 and IGF2BP2 in cervical cancer (CaSki) cells. CircARHGAP12 was labeled with the FAM (green) and IGF2BP2 was labeled with the cy3 (red). **D, E** Biotin-labeled RNA pull-down was performed using circARHGAP12 probe and control probe. The enrichment of circARHGAP12 was measured using RT-qPCR and the level of IGF2BP2 protein was detected using western blot assay. Experiments were performed in triplicate. *P* values were calculated by Student's *t*-test. ***p* < 0.01.

DISCUSSION

Cervical cancer acts as one of the most common gynecologic cancers, and increasing evidence suggests the emerging role of circRNAs in cervical cancer tumorigenesis [16, 17]. Moreover, the regulation of m⁶A in cervical cancer catches researchers' attention. Here, we focused on the function of m⁶A-circRNAs on cervical cancer.

With the aid of circRNA high-throughput sequencing, we found that a novel circRNA circARHGAP12 was upregulated in the cervical cancer tissue and adjacent normal tissue. CircARHGAP12 (hsa_circ_0000231, 794 bp) was generated from the exon 3 and exon 2 of the ARHGAP12 gene. Interestingly, there was an m⁶A modification site in exon 3, indicating the potential m⁶A-circRNA interaction in the circARHGAP12. The special m⁶A modification in the circARHGAP12 clue that the biogenesis or biological

characteristic of circARHGAP12 may be varied due to the m⁶A. Subsequently, we discovered that m⁶A reader IGF2BP2 could recognize the m⁶A site in circARHGAP12 and meanwhile enhance its enrichment. Existing researches revealed that m⁶A reader could specifically combine with circRNA to regulate the circRNA fate. For instance, in human immunity, m⁶A modification receded the immune gene activation and adjuvant activity, and m⁶A reader YTHDF2 is essential for suppression of innate immunity through sequestering the m⁶A-circRNA [18]. Another m⁶A reader YTHDC1 connects with m⁶A-modified circ-ARL3, which sponges miR-1305 and thereby promotes HBV+ HCC progression [19]. Therefore, these evidences clue that m⁶A modification could regulate the function of circRNAs.

Functionally, the biofunctional assays found that circARHGAP12 could promote the proliferation and migration of cervical cancer

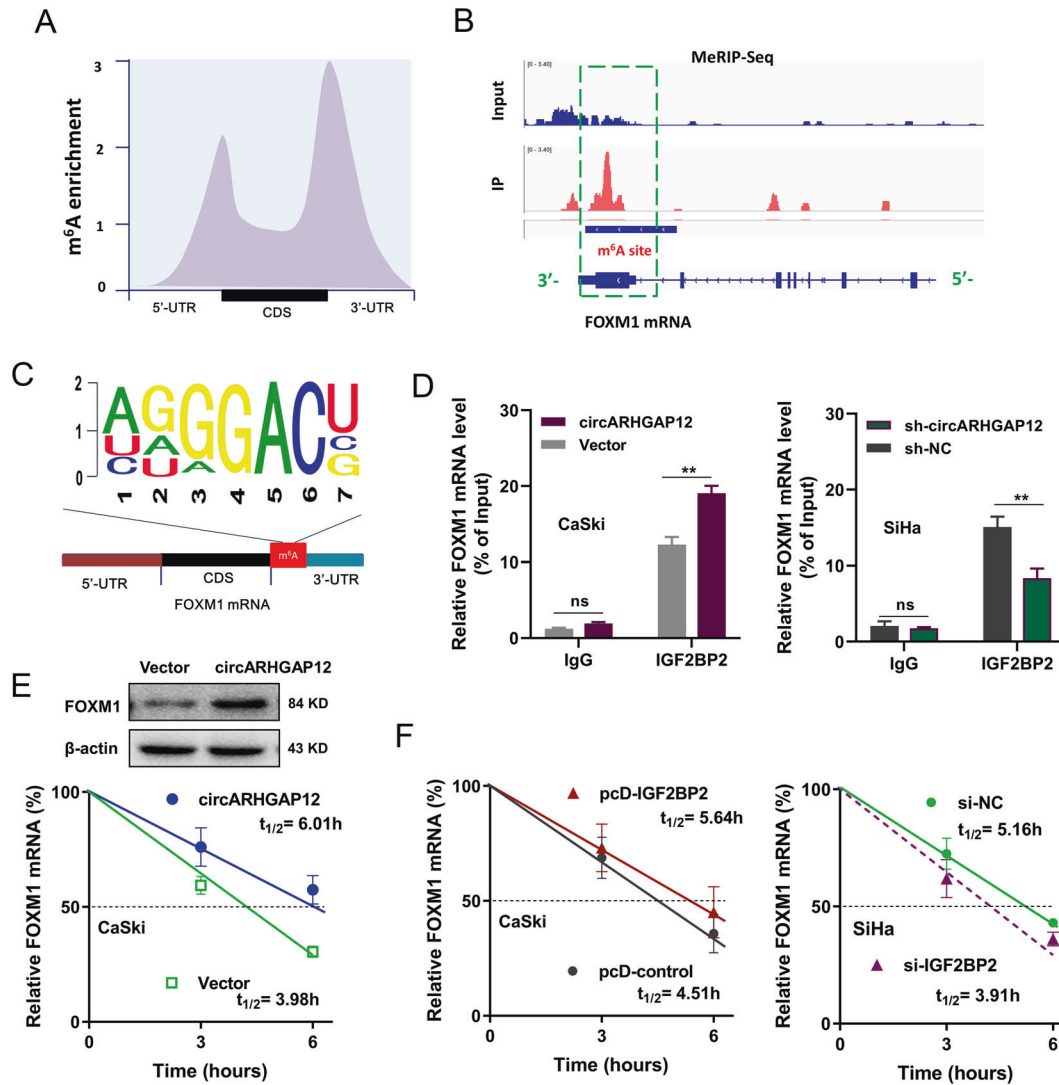


Fig. 5 circARHGAP12/IGF2BP2 enhanced the stability of FOXM1 mRNA. **A** MeRIP-Seq was performed to discover the potential m⁶A modification profile in the cervical cancer cells. m⁶A sites were displayed in 5'-UTR, 3'-UTR, and CDS. **B** Schematic diagram based on MeRIP-Seq showed the remarkable m⁶A modification site in the 3'-UTR of FOXM1 mRNA. **C** Symbol showed the m⁶A motif in the FOXM1 mRNA (GGACU). **D** RBP immunoprecipitation (RIP)-qPCR assay demonstrated the FOXM1 mRNA enrichment precipitated by anti-IGF2BP2 antibody in CaSki or SiHa cells transfected with circARHGAP12 (plasmids) overexpression or circARHGAP12 knockdown (sh-circARHGAP12). IgG acted as the blank control. **E** RNA stability assay and western blot assay demonstrated the FOXM1 mRNA and protein level in CaSki cells transfected with circARHGAP12 overexpression. **F** RNA stability assay showed the FOXM1 mRNA expression in CaSki cells transfected with IGF2BP2 overexpression (pcD-IGF2BP2), or in SiHa cells transfected with IGF2BP2 silencing (si-IGF2BP2). Experiments were performed in triplicate. *P* values were calculated by Student's *t*-test. ***p* < 0.01.

cells (CaSki, SiHa). Besides, *in vivo* experiments demonstrated that circARHGAP12 accelerated the tumor growth of cervical cancer cells. In the enormous number of circRNAs, circARHGAP12 is a novel identified circRNAs and its functions have been described. For example, in DOX-induced cardiotoxicity, circArhgap12 is upregulated in the mouse heart tissue, and circArhgap12 could sponge miR-135a-5p to regulate ADCY1 mRNA in rat primary cardiomyocytes [20]. In nasopharyngeal carcinoma, circARHGAP12 is significantly upregulated and regulates the expression of cytoskeletal remodeling-related proteins (EZR, TPM3, and RhoA) through directly binding the mRNA 3'-UTR and promoting its stability via EZR/TPM3/RhoA complex [21]. Thus, these data demonstrates the biological role of circARHGAP12.

Subsequently, we found that circARHGAP12 interacted with m⁶A reader IGF2BP2 through m⁶A site in the exon-3, one of the elements of circARHGAP12. Subcellular co-localization assay found that circARHGAP12 and IGF2BP2 were collectively located in the

cytoplasm. Based on the MeRIP-Seq data, we found that there was a remarkable m⁶A modification site in the 3'-UTR of FOXM1 mRNA. CircARHGAP12 improves the FOXM1 mRNA enrichment precipitated by an anti-IGF2BP2 antibody. In other words, circARHGAP12 interacts with IGF2BP2 to combine with FOXM1, forming circARHGAP12/IGF2BP2/FOXM1 complex (Fig. 6). In cervical cancer, FOXM1 was found to be an oncogene [22]. Thus, this regulation pathway might reveal the oncogenic route for cervical cancer.

Collectively, these findings provide robust evidence that novel circRNA circARHGAP12 acts as an oncogene in cervical cancer tumorigenesis. m⁶A-modified circARHGAP12 interacts with IGF2BP2 to enhance FOXM1 mRNA stability, forming circARHGAP12/IGF2BP2/FOXM1 complex, thereby promoting the proliferation and migration of cervical cancer cells. These achievements might provide solving ideas for the targeted therapy with a view to the m⁶A-circRNA approach.

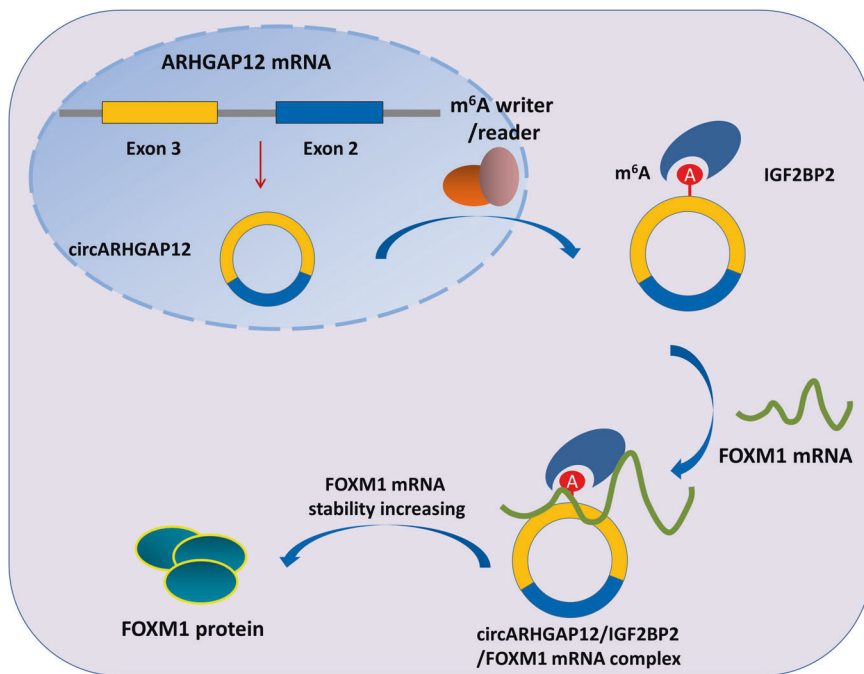


Fig. 6 m⁶A-modified circARHGAP12 promotes cervical cancer progression by enhancing FOXM1 mRNA stability via interacting IGF2BP2.

MATERIALS AND METHODS

Clinical patients' tissue specimen collection

The cervical cancer patients' tissue specimens (forty-eight cases) were recruited during the surgery. All the volunteers had been informed of the clinical recruitment and understood the experimental procedure. Informed consent was acquired from every patient. Cancer tissue and paired adjacent non-tumor tissues were collected and reserved under -80°C . The procedures were approved by the Ethics Committee of Shenzhen Baoan Women's and Children's Hospital.

Cervical cancer cells and transfection

The human epidermal cell (HaCaT) and cervical cancer cell lines (HT-3, CaSki, C33A, and SiHa) were provided from the Chinese Academy of Sciences Cell Bank (Shanghai, China). Cells were cultured in RPMI 1640 medium (Invitrogen, Carlsbad, CA) with 10% fetal bovine serum (FBS), 100 $\mu\text{g}/\text{mL}$ streptomycin, and 100 U/mL penicillin G at 37°C in a 5% CO_2 atmosphere. Lentivirus plasmids of shRNA were constructed by Genechem Company (Shanghai, China) and packaged using pMD2.G and psPAX2 (Addgene, Cambridge, MA) into cell. After transfection, virus supernatants were concentrated to infect cervical cancer cells by polybrene (8 $\mu\text{g}/\text{mL}$, Sigma, MO). Three days later, cells were treated with puromycin (2 $\mu\text{g}/\text{mL}$, Sigma) for 7 days. For circARHGAP12 overexpression, RNA was amplified from reverse-transcribed cDNA and the PCR products were cloned into the pZW1-FCS-circRNA vector (Addgene).

Quantitative real-time polymerase chain reaction (qRT-PCR)

The total RNA was isolated from cervical cancer cells or tissue samples using Trizol reagent. Total RNA (0.5 μg) was used for reverse transcription for cDNA. Reverse transcription was performed by HiScript Q RT-SuperMix for qPCR (Vazyme, China). PCR was performed using SYBR Green PCR kit (TaKaRa, Dalian, China) on Applied Biosystems 7300 detection system (Applied Biosystems) with triplicate times. All these primers were listed in Supplementary Table S1.

m⁶A quantitative analysis

Firstly, the total RNA was extracted from cervical cancer cells using TRIzol following the manufacturer's protocol. The global m⁶A level in total mRNA was detected through the colorimetric EpiQuik m⁶A RNA Methylation Quantification Kit (Epigentek) according to the manufacturer's instructions. The m⁶A enrichment was colorimetrically detected using the 450 nm absorbance.

RNase R and actinomycin D treatment

For RNase R treatment assay, 2 mg of total RNA was incubated with or without 5 U/ μg RNase R (Epicentre Technologies, Madison WI, USA) at 37°C for 30 min. Then, RNA was purified using RNeasy MinElute Cleaning Kit (Qiagen) and subsequently calculated by qRT-PCR. For Actinomycin D (Act D) treatment assay, cells (5×10^5 cells/well) were seeded in six-well plates and then exposed to 2 $\mu\text{g}/\text{mL}$ Actinomycin D (Sigma). At indicated time points, cells were collected and the RNA stability was analyzed using qRT-PCR normalizing to mock treatment group.

Methylated RNA immunoprecipitation PCR (MeRIP-PCR)

For the quantitative analysis of m⁶A-modified mRNA, MeRIP-PCR was performed. After the isolation of mRNA, anti-m⁶A antibody and anti-IgG (Cell Signaling Technology) were conjugated with protein A/G magnetic beads in IP buffer (140 mM NaCl, pH 7.5 20 mM Tris, 2 mM EDTA, 1% NP-40, RNase inhibitor, and protease inhibitor) at 4°C overnight. After incubation, the RNA-beads complex was eluted using elution buffer. Lastly, the RNA enrichment was identified using the qRT-PCR assay calculating the $2^{-\Delta\Delta\text{Ct}}$ of eluate relative to the input sample.

Proliferation assay

Proliferation ability was detected using CCK-8 assay and colony formation assay. For the CCK-8 assay, the transfected cervical cancer cells were added with a cell counting kit-8 (CCK-8) reagent (Dojindo, Japan, 10 mL/well). The optical density (OD) value was detected at 450 nm by an enzyme-mark reader. For colony formation assay, the transfected cervical cancer cells were seeded in the fresh six-well plate in 1640 medium containing 10% FBS. After 14 days, cells were fixed with methanol and stained with crystal violet (0.1%). Lastly, colonies were manually counted.

Western blot analysis

Total protein in cells was extracted using radioimmunoprecipitation assay (RIPA) buffer containing PMSF (phenylmethanesulfonyl fluoride). After centrifugation (10 min, 4°C , 25,764 $\times g$), the supernatant was collected. The concentration of protein in the sample was detected using bicinchoninic acid (BCA) kit and then adjusted by deionized water. SDS-PAGE (10%) was configured for protein separation and then transferred to PVDF (polyvinylidene fluoride) membrane (Millipore). The membranes were administrated with 5% skimmed milk for 2 h and then incubated with primary antibody anti-FOXM1 (1:1000, Abcam, ab207298), rabbit anti-IGF2BP2 (1:1000, Abcam, ab124930), β -actin (1:2000, ab8226, Abcam) at 4°C overnight. After being washed with PBS tween-20 (PBST) three times,

the membrane was immersed in enhanced chemiluminescence (ECL) reaction solution for images exposure.

Fluorescence in situ hybridization (FISH)

The subcellular location of circARHGAP12 and IGF2BP2 was detected using the FISH assay. In brief, FAM-labeled circARHGAP12 probes, Cy3-labeled IGF2BP2 probes, and DAPI-labeled probes were provided by Genepharma (Shanghai, China). Nuclei was stained by 4,6-diamidino-2-phenylindole (DAPI). The FISH assay was performed using a fluorescent in situ hybridization kit (Genepharma) according to the manufacturer's protocol. Images were captured with a confocal microscope (Olympus).

RNA immunoprecipitation (RIP) assay

RIP assay was performed for the RNA-protein interaction using MagnaRIP RNA-Binding Protein Immunoprecipitation Kit (Millipore, MA, USA) according to the manufacturer's instructions. In brief, cell lysates were extracted from cervical cancer cells. RNA were incubated with antibody-coated buffer containing beads (anti-IGF2BP2, control rabbit IgG, Abcam) at 4 °C overnight. The conjugated precipitation was eluted and detected using qRT-PCR analysis.

RNA pull-down assay

Biotin-labeled circARHGAP12 probe RNA pull-down assay was synthesized by Genepharma (Shanghai, China). Cervical cancer cells were lysed and incubated with specific probes and streptavidin-coated magnetic beads in a lysis buffer. The biotin-labeled RNA complex was pulled down and the beads were washed and purified. Then, the enrichment of circARHGAP12 was analyzed by qRT-PCR, and the retrieved IGF2BP2 protein was detected using a western blot.

Mice xenograft model assay

In vivo animal experiments were approved by the Ethics Committee of Shenzhen Baoan Women's and Children's Hospital. Ten BALB/c nude mice (male, 15 g) were purchased from the SLAC Laboratory Animal Center (Shanghai, China). CircARHGAP12-stable knockdown cervical cancer cells (100 μ L PBS containing 5×10^6 cells) were subcutaneously injected into the lateral flank of BALB/c nude mice. The length and width were measured every 3 days to calculate the tumor volume. Mice were sacrificed after 4 weeks and the tumor was weighed. The injection was randomly performed.

Statistical analysis

The statistical analysis was performed by GraphPad Prism v7.0 software. All functional experiments were performed for triplicate times and data was displayed as means \pm SD (standard deviation). Student's *t*-test and ANOVA were used to compare the statistical significance within two groups and differences between groups. Among them, $p < 0.05$ or $p < 0.01$ was considered statistical significant.

REFERENCES

- Liu Y, Li L, Li Y, Zhao X. Research progress on tumor-associated macrophages and inflammation in cervical cancer. *BioMed Res Int.* 2020;2020:6842963.
- Marchetti C, Fagotti A, Tombolini V, Scambia G, De Felice F. Survival and toxicity in neoadjuvant chemotherapy plus surgery versus definitive chemoradiotherapy for cervical cancer: a systematic review and meta-analysis. *Cancer Treat Rev.* 2020;83:101945.
- Shen S, Zhang S, Liu P, Wang J, Du H. Potential role of microRNAs in the treatment and diagnosis of cervical cancer. *Cancer Genet.* 2020;248–249:25–30.
- Han B, Chao J, Yao H. Circular RNA and its mechanisms in disease: from the bench to the clinic. *Pharmacol Ther.* 2018;187:31–44.
- Hsiao KY, Sun HS, Tsai SJ. Circular RNA - New member of noncoding RNA with novel functions. *Exp Biol Med.* 2017;242:1136–41.
- Tornesello ML, Faraonio R, Buonaguro L, Annunziata C, Starita N, Cerasuolo A, et al. The role of microRNAs, long non-coding RNAs, and circular RNAs in cervical cancer. *Front Oncol.* 2020;10:150.
- Huang A, Zheng H, Wu Z, Chen M, Huang Y. Circular RNA-protein interactions: functions, mechanisms, and identification. *Theranostics.* 2020;10:3503–17.
- Li J, Guo R, Liu Q, Sun J, Wang H. Circular RNA Circ-ITCH inhibits the malignant behaviors of cervical cancer by microRNA-93-5p/FOXK2 Axis. *Reprod Sci.* 2020;27:860–8.
- Yue B, Song C, Yang L, Cui R, Cheng X, Zhang Z, et al. METTL3-mediated N6-methyladenosine modification is critical for epithelial-mesenchymal transition and metastasis of gastric cancer. *Mol Cancer.* 2019;18:142.

- Hu X, Peng WX, Zhou H, Jiang J, Zhou X, Huang D, et al. IGF2BP2 regulates DANCER by serving as an N6-methyladenosine reader. *Cell Death Differ.* 2020;27:1782–94.
- Hu Y, Ouyang Z, Sui X, Qi M, Li M, He Y, et al. Oocyte competence is maintained by m(6)A methyltransferase KIAA1429-mediated RNA metabolism during mouse follicular development. *Cell Death Differ.* 2020;27:2468–83.
- He L, Li H, Wu A, Peng Y, Shu G, Yin G. Functions of N6-methyladenosine and its role in cancer. *Mol Cancer.* 2019;18:176.
- Ma S, Chen C, Ji X, Liu J, Zhou Q, Wang G, et al. The interplay between m6A RNA methylation and noncoding RNA in cancer. *J Hematol Oncol.* 2019;12:121.
- Wang Q, Guo X, Li L, Gao Z, Su X, Ji M, et al. N(6)-methyladenosine METTL3 promotes cervical cancer tumorigenesis and Warburg effect through YTHDF1/HK2 modification. *Cell Death Dis.* 2020;11:911.
- Li Z, Peng Y, Li J, Chen Z, Chen F, Tu J, et al. N(6)-methyladenosine regulates glycolysis of cancer cells through PDK4. *Nat Commun.* 2020;11:2578.
- Chaichian S, Shafabakhsh R, Mirhashemi SM, Moazzami B, Asemi Z. Circular RNAs: a novel biomarker for cervical cancer. *J Cell Physiol.* 2020;235:718–24.
- Tang Q, Chen Z, Zhao L, Xu H. Circular RNA hsa_circ_0000515 acts as a miR-326 sponge to promote cervical cancer progression through up-regulation of ELK1. *Aging.* 2019;11:9982–99.
- Wang Y, Lu JH, Wu QN, Jin Y, Wang DS, Chen YX, et al. LncRNA LINRIS stabilizes IGF2BP2 and promotes the aerobic glycolysis in colorectal cancer. *Mol Cancer.* 2019;18:174.
- Rao X, Lai L, Li X, Wang L, Li A, Yang Q. N(6)-methyladenosine modification of circular RNA circ-ARL3 facilitates Hepatitis B virus-associated hepatocellular carcinoma via sponging miR-1305. *IUBMB Life.* 2021;73:408–17.
- Wang X, Cheng Z, Xu J, Feng M, Zhang H, Zhang L, et al. Circular RNA Arhgap12 modulates doxorubicin-induced cardiotoxicity by sponging miR-135a-5p. *Life Sci.* 2021;265:118788.
- Fan C, Qu H, Xiong F, Tang Y, Tang T, Zhang L, et al. CircARHGAP12 promotes nasopharyngeal carcinoma migration and invasion via ezrin-mediated cytoskeletal remodeling. *Cancer Lett.* 2021;496:41–56.
- Hong H, Zhu H, Zhao S, Wang K, Zhang N, Tian Y, et al. The novel circCLK3/miR-320a/FoxM1 axis promotes cervical cancer progression. *Cell Death Dis.* 2019;10:950.

ACKNOWLEDGEMENTS

This work was supported by intra-hospital fund of Shenzhen Baoan Women's and Children's Hospital (BAFY 2020003), Shenzhen Key Medical Discipline Construction Fund (No. SZXK028), Shenzhen Science and Technology Innovation Committee Foundation (JCYJ20190809185001766).

AUTHOR CONTRIBUTIONS

F.J. and Y.L. are the major performers for this study. S.C., Y.Y., and Xiaoling Lin and are the assists for statistic analysis and literature novelty. Y. Z. and Xin Luo is the response to the design and funding.

COMPETING INTERESTS

The authors declare no competing interests.

ETHICS STATEMENT

All experiments were approved by the Ethics Committee of Shenzhen Baoan Women's and Children's Hospital.

ADDITIONAL INFORMATION

Supplementary information The online version contains supplementary material available at <https://doi.org/10.1038/s41420-021-00595-w>.

Correspondence and requests for materials should be addressed to Y.Z. or X.L.

Reprints and permission information is available at <http://www.nature.com/reprints>

Publisher's note Springer Nature remains neutral with regard to jurisdictional claims in published maps and institutional affiliations.



Open Access This article is licensed under a Creative Commons Attribution 4.0 International License, which permits use, sharing, adaptation, distribution and reproduction in any medium or format, as long as you give appropriate credit to the original author(s) and the source, provide a link to the Creative Commons license, and indicate if changes were made. The images or other third party material in this article are included in the article's Creative Commons license, unless indicated otherwise in a credit line to the material. If material is not included in the

article's Creative Commons license and your intended use is not permitted by statutory regulation or exceeds the permitted use, you will need to obtain permission directly from the copyright holder. To view a copy of this license, visit <http://creativecommons.org/licenses/by/4.0/>.

© The Author(s) 2021